The Analysis of a Coaxial-to-Waveguide Transition Using FDTD with Cylindrical to Rectangular Cell Interpolation Scheme

Kyung-Wan Yu[a], Sung-Choon Kang, Hee-Jin Kang, Jae-Hoon Choi, and Jin-Dae Kim

We analyze the characteristics of a coaxial-to-waveguide transition based on the finite difference time domain (FDTD) method with the cylindrical to rectangular cell interpolation scheme. The scheme presented in this paper is well suited for the analysis of a microwave device with a probe near waveguide discontinuity because perfect TEM mode can be generated inside the coaxial cable by using the cylindrical cell. The scattering parameters of a designed Ka-band transition are evaluated and compared with those of commercially available software, High Frequency Structure analysis Simulator (HFSS) and measured data. There exists good agreement between the measured and calculated data. In order to prove an accuracy of the interpolation scheme, a coaxial to waveguide transition with a disk-loaded probe is analyzed by the present approach and the results of this analysis are compared with measured data. Comparison shows that our results match very closely to those of measurement and other approaches. The method presented in this paper can be applied to analyze the characteristics of a probe excited cavity, coaxial waveguide T-Junctions, and so on.

Manuscript received August 7, 1998; revised March 22, 1999.
This work is supported in part by ETRI.
a)Electronic mail: kwyu@etri.re.kr

I. INTRODUCTION

Modern satellite communication payload systems call for high performance microwave devices. Among those devices, a coaxial-to-waveguide transition is very useful to transfer the microwave signal from one structure to another. The transition structure can be applied in modern communication devices, such as power dividers, bandpass filters, manifold multiplexers, or couplers. In this paper, a Ka-band coaxial to waveguide transition is analyzed using FDTD with cell interpolation scheme.

Over the years many researchers have applied various analysis methods to predict the accurate performance characteristics of similar structures. Two most commonly investigated structures of coaxial probe in rectangular waveguide are coaxial line-waveguide T-junction and coaxial line-waveguide transition. Variational method and image method were used to obtain the input impedance of a coaxial probe protruding into the rectangular waveguide by assuming a single mode current located at the center of a probe [1], [2]. However, this assumption leads to inaccurate results for a thick probe.

The FDTD method is introduced by Yee in 1966 [3] and has been successfully applied for analyzing the characteristics of various microwave problems such as waveguide, multilayer structures, discontinuities, filters, and antennas. Recently Navarro analyzed the characteristics of a T-junction [4] and patch antenna [5] consisting of a rectangular coaxial cable using the FDTD method [6]−[7]. In his analysis, a rectangular coaxial cable, which is not

commonly used in real situation, was used instead of a circular coaxial cable. Additionally John M. Jarem [8] calculated the input impedance of a probe sleeve fed rectangular waveguide cavity which was short circuited on one side by using the multifilament method of moments (MOM) and the FDTD method. Paul Y. Chung [9] used a circular mesh scheme for the non-orthogonal FDTD method to evaluate the s-parameters of a rat-race coupler.

Several methods can be used to analyze a coaxial-to-waveguide transition based on the finite difference time domain (FDTD) method. By dividing the whole calculation region into very small uniform cells, the accuracy of the FDTD technique can be improved. However, the usage of very small cell requires the huge computer memory and calculation time. The subcell method suggested by Michal Okoniewski [10] can provide the versatility but dispersion problem can be generated. Most of all, perfect TEM mode inside a coaxial cable can be hardly obtained by the upper mentioned two methods.

In this paper, a new approach, which utilizes the Taylor series and coordinate transformation technique, is applied to transform the rectangular coordinate grid data to cylindrical coordinate data and vice versa at the interface between the regular rectangular FDTD cells and the cylindrical FDTD cells. The TEM wave is generated in coaxial cable by the cylindrical FDTD method. In the region, where the inner conductor of a coaxial cable protruding into rectangular waveguide, the FDTD with cylindrical to rectangular cell interpolation scheme is used for the smooth transition of electromagnetic fields from rectangular cell to cylindrical cell and vice versa. As an example, s-parameters of a coaxial to waveguide transition with and without disk loading are evaluated by FDTD with the interpolation scheme suggested in this paper.

To verify the accuracy of the present approach, s-parameters of an analyzed transition are compared with those of HFSS [11] and measured data [12], [13]. The computed results and measured data agree very well in most of the frequency band of interest.

II. THEORETICAL APPROACH

1. Basic Equations of FDTD

Electromagnetic fields in time domain are satisfying the following Maxwells equations:

$$\triangle \times \vec{E} = -\mu \frac{\partial \vec{H}}{\partial t} - \rho_m \vec{H} \quad , \tag{1a}$$

$$\triangle \times \vec{H} = \varepsilon \frac{\partial \vec{E}}{\partial t} + \sigma \vec{E}, \tag{1b}$$

$$\triangle \cdot \vec{D} = \rho^* \ , \tag{1c}$$

$$\triangle \cdot \vec{B} = 0 \ , \tag{1d}$$

where permeability μ, conductivity σ, permittivity ε, electric charge density ρ^* and an equivalent magnetic resistivity ρ_m are time independent real quantities. $\vec{E}$, $\vec{D}$, $\vec{H}$ and $\vec{B}$ represent the electric field, electric flux density, magnetic field, and magnetic flux density vectors, respectively.

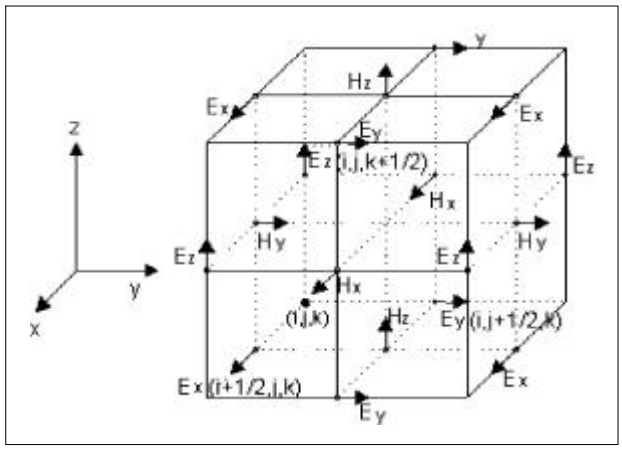

Fig. 1. Yee cell of the rectangular coordinate system.

The vector curl equations (1a) and (1b) can be written in scalar equation either by rectangular coordinate system or by cylindrical coordinate system. Following Yee's notation [3] shown in Fig. 1, a point (i, j, k) in the FDTD mesh is representing $(i\triangle x, j\triangle y, k\triangle z)$ in rectangular coordinates and $(i\triangle\rho, j\triangle\phi, k\triangle z)$ in cylindrical coordinates. By using this notation, any function F of space and time can be denoted as

$$F^n(i,j,k) = F(i\triangle x, j\triangle y, k\triangle z, n\triangle t) \quad , \tag{2}$$

where $\triangle x, \triangle y, \triangle z$ are representing incremental step sizes in x, y, z directions, respectively and $\triangle t$ is time step size.

Equation (1a) can be written in finite difference equation for the HZ by using the notation in (2) as

$$H_z\big|^{n+1/2}_{i+1/2,j+1/2,k} = H_z\big|^{n-1/2}_{i+1/2,j+1/2,k} + \frac{\triangle t}{\mu}\left[\frac{E_x\big|^n_{i+1/2,j+1,k} - E_x\big|^n_{i+1/2,j,k}}{\triangle y} - \frac{E_y\big|^n_{i+1,j+1/2,k} - E_y\big|^n_{i,j+1/2,k}}{\triangle x}\right] \quad . \tag{3}$$

In a similar manner, we can derive finite difference expressions for the remaining components. The finite difference equations in cylindrical coordinate system can also be written in similar manner.

The accuracy of the solution is affected by the choice of space and time steps used. The space incremental step size must be a small fraction of wavelength and the overall dimension of a structure. The time incremental size sould satisfy the following stability condition [6]:

$$v_{\max}\Delta t \leq \left(\frac{1}{\Delta\rho^2}+\frac{1}{(\rho_{\min}\Delta\phi)^2}+\frac{1}{\Delta z^2}\right)^{-\frac{1}{2}}, \quad (4)$$

where v_{max} is the maximum phase velocity in the model and $\rho_{min}\nabla\phi$ is minimum grid size in ϕ direction.

2. Transformation between the Rectangular and Cylindrical Coordinates

In applying FDTD to a coaxial to waveguide transition, a usual rectangular or polygonal cell modeling is not suitable for accurate analysis. Therefore, the structure under consideration needs a modified FDTD algolithm. The structure under investigation is subdivided into three regions as shown in Fig. 2.

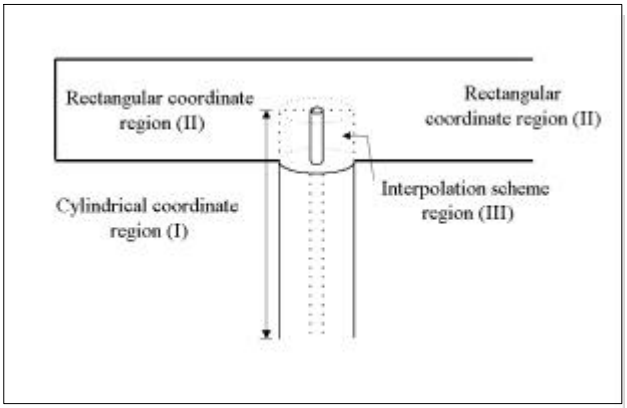

Fig. 2. Cross sectional view of a transition under study.

In the first region (coaxial cable region), finite difference equations in cylindrical coordinate system are used and the rectangular coordinate finite difference equations are used in the second region (waveguide region). Finally, for the analysis of the field in the region III (interpolation scheme region), where the inner conductor of a coax protruding into the rectangular waveguide, the first order Taylar series expansion and coordinate transformation scheme are adopted for the smooth transition of electromagnetic fields from rectangular cells to cylindrical cells.

A. Data Transformation from the Cylindrical Coordinates to Rectangular Coordinates

As shown in Fig. 3, the point Q of a rectangular cell can be represented in terms of ρ and ϕ of cylindrical coordinate system with respect to origin 'O'.

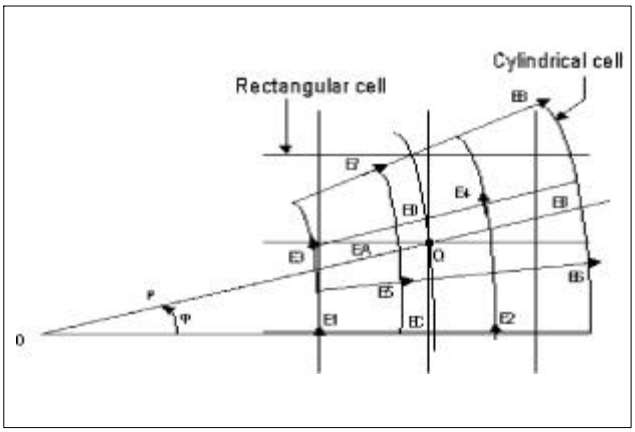

Fig. 3. Cylindrical-to-rectangular interpolation scheme.

Field components surrounding point $Q(x,y)$ are given by

$$E1 = E_\phi(IR', I\Phi'), \quad E5 = E_\rho(IR, I\Phi),$$
$$E2 = E_\phi(IR'+1, I\Phi'), \quad E6 = E_\rho(IR+1, I\Phi),$$
$$E3 = E_\phi(IR', I\Phi'+1), \quad E7 = E_\rho(IR, I\Phi+1),$$
$$E4 = E_\phi(IR'+1, I\Phi'+1), \quad E8 = E_\rho(IR+1, I\Phi+1),$$

where $E\phi(i, j)$ is a ϕ component of an electric field at (i, j)th grid point and $E\rho(k, l)$ is a ρ component at (k, l)th grid point.

By using the first order Taylor series expansion, fields at EA and EB can be represented approximately as

$$EA = E_\rho(IR, I\Phi) + f_1 \times (\rho - I\Phi\Delta\rho)(IR+0.5)\Delta\rho, \quad (5a)$$

where $$f_1 = \frac{E_\rho(IR, I\Phi+1) - E_\rho(IR, I\Phi)}{(IR+0.5)\Delta\rho\Delta\rho}, \quad (5b)$$

and

$$EB = E_\rho(IR+1, I\Phi) + f_2 \times (\rho - I\Phi\Delta\rho)(IR+1.5)\Delta\rho, \quad (6a)$$

where $$f_2 = \frac{E_\rho(IR+1, I\Phi+1) - E_\rho(IR+1, I\Phi)}{(IR+1.5)\Delta\rho\Delta\rho}. \quad (6b)$$

The ρ component of the electric field at Q is given in terms of EA and EB as

$$E_{\rho} = EA + f_3 \times (\rho - (IR + 0.5)\triangle\rho) \quad , \tag{7a}$$

where $f_3 = \dfrac{EB - EA}{\triangle\rho}$, (7b)

$$EC = E_{\phi}(IR', I\Phi') + f_4 \times (\rho - IR'\triangle\rho) \quad , \tag{8a}$$

where $f_4 = \dfrac{E_{\rho}(IR'+1, I\Phi') - E_{\phi}(IR', I\Phi')}{\triangle\rho}$, (8b)

and

$$ED = E_{\phi}(IR', I\Phi'+1) + f_5 \times (\rho - IR'\triangle\rho) \quad , \tag{9a}$$

where $f_5 = \dfrac{E_{\phi}(IR'+1, I\Phi'+1) - E_{\phi}(IR', I\Phi'+1)}{\triangle\rho}$. (9b)

The ϕ component of the electric field at Q can be represented using EC and ED as

$$\mathbf{E}_{\phi} = \mathbf{E}C + f_6 \times (\phi - (I\Phi' + 0.5)\triangle\phi)\rho \quad , \tag{10a}$$

where $f_6 = \dfrac{ED - EC}{\rho\triangle\phi}$. (10b)

Once the ρ and ϕ components of the field at Q are obtained, these components can be transformed into the rectangular coordinate system as

$$E_x = E_{\rho}(\rho, \phi)\cos\phi - E_{\phi}(\rho, \phi)\sin\phi \quad , \tag{11a}$$

and

$$E_y = E_{\rho}(\rho, \phi)\sin\phi + E_{\phi}(\rho, \phi)\cos\phi \quad . \tag{11b}$$

B. Data Transformation from the Rectangular Coordinate to Cylindrical Coordinate

The rectangular cell to cylindrical cell interpolation scheme is necessary for the calculation of field values at the outermost cell of cylindrial coordinate.

The field components surrounding the point $Q(x,y)$ in Fig. 4 are given by

$$E1 = E_x(IX, IY) \quad , \qquad E5 = E_y(IX', IY') \quad ,$$

$$E2 = E_x(IX+1, IY) \quad , \qquad E6 = E_y(IX'+1, IY') \quad ,$$

$$E3 = E_x(IX, IY+1) \quad , \qquad E7 = E_y(IX', IY'+1) \quad ,$$

$$E4 = E_x(IX+1, IY+1) \quad , \qquad E8 = E_y(IX', IY'+1) \quad .$$

By adopting the first order Taylor series approximation, fields at EA and EB are given by

$$EA = E_x(IX, IY) + f_1 \times (x - (IX + 0.5)\triangle x) \quad , \tag{12a}$$

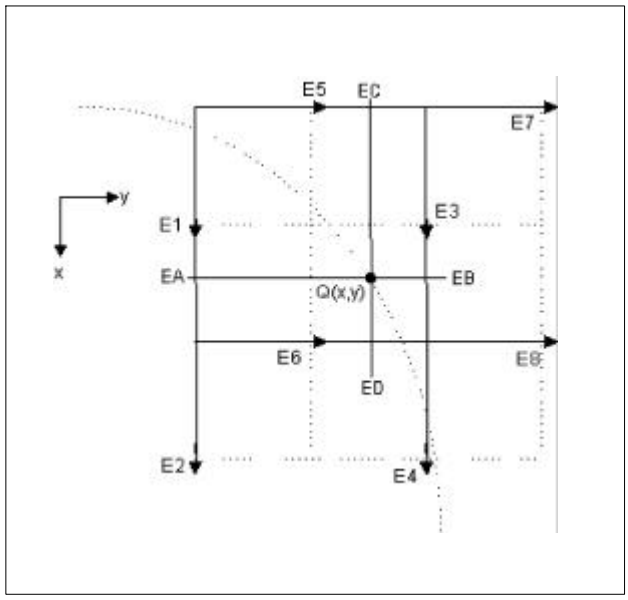

Fig. 4. Rectangular-to-cylindrical interpolation scheme.

where $f_1 = \dfrac{E_x(IX+1, IY) - E_x(IX, IY)}{\triangle x}$, (12b)

and

$$EB = E_x(IX, IY+1) + f_2 \times (x - (IX + 0.5)\triangle x) \quad , \tag{13a}$$

where $f_2 = \dfrac{E_x(IX+1, IY+1) - E_x(IX, IY+1)}{\triangle x}$. (13b)

The x component of the electric field at Q can be written in terms of EA and EB as

$$E_x = EA + f_3 \times (y - IY\triangle y) \quad , \tag{14a}$$

where $f_3 = \dfrac{EB - EA}{\triangle y}$, (14b)

$$EC = E_y(IX', IY') + f_4 \times (y - (IY' + 0.5)\triangle y) \quad , \tag{15a}$$

where $f_4 = \dfrac{E_y(IX', IY'+1) - E_y(IX', IY')}{\triangle y}$, (15b)

and

$$ED = E_y(IX'+1, IY') + f_5 \times (y - (IY' + 0.5)\triangle y) \tag{16a}$$

where $f_5 = \dfrac{E_y(IX'+1, IY'+1) - E_y(IX'+1, IY')}{\triangle y}$. (16b)

The y component of the electric field at Q is given by

$$E_y = EC + f_6 \times (x - IX'\triangle x) \quad , \tag{17a}$$

where $f_6 = \dfrac{ED - EC}{\triangle x}$. (17b)

One can represent the electrical field components in

cylindrical coordinate system from *Ex* and *Ey* given in equation (14a) and (17a) as

$$E_{\phi} = E_x(x,y)\cos\phi + E_y(x,y)\sin\phi \tag{18a}$$

and

$$E_{\phi} = -E_x(x,y)\sin\phi + E_y(x,y)\cos\phi. \tag{18b}$$

Ez and *H* field components can be obtained in similar manner.

3. Incident Field and Scattering Parameters

A. Source Modeling

The Gaussain pulse given in equation (19) is applied at the end of a coaxial cable to obtain the frequency characteristics of a designed transition.

$$E_{\phi}|_{in} = \frac{V_0}{\phi \ln(b/a)} \exp(-\alpha(t-\beta\Delta t)^2) \quad , \tag{19}$$

where *a* and *b* are the inner and outer radii of a coaxial cable, ρ is the distance from the center of a coax and β is the number of time steps used for the Gaussain pulse from the peak to the truncated value.

B. Calculation of Scattering Parameters

The incident and reflected field values at the terminal plane for different time steps are saved and discrete Fourier transform are performed to obtain field values in frequency domain. From these frequency field values, s-parameters are evaluated as

$$S_{11}(f) = \frac{V_{ref}(f)}{V_{inc}(f)} = \frac{\int_a^b E_{ref}(f,\phi')\,d\phi'}{\int_a^b E_{inc}(f,\phi')\,d\phi'} \quad , \tag{20}$$

where *a* and *b* are inner and outer radii of a coaxial cable, respectively. $E_{inc}(f,\rho')$ and $E_{ref}(f,\rho')$ are the incident and reflected electric fields in frequency domain. ρ' is the distance parameter in the usual cylindrical coordinate system. *S*21 is obtained from *S*11 as [14]

$$|S_{21}(f)| = \sqrt{1-|S_{11}(f)|^2} \quad . \tag{21}$$

III. NUMERICAL RESULTS

Coaxial to waveguide transitions are designed and analyzed using the method described in the previous chapter. For the verification purpose, results of present approach are compared with those of HFSS and measured data for three different transition structures.

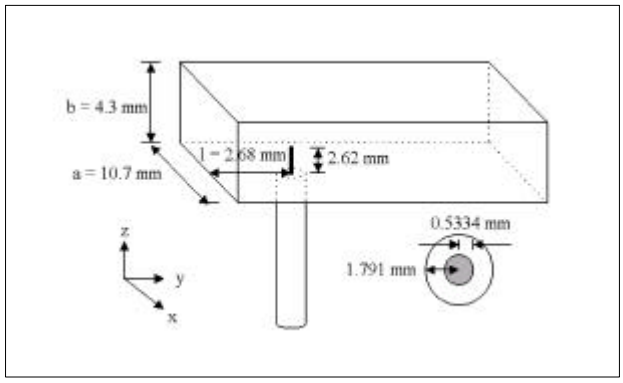

Fig. 5. Structure of a coaxial to waveguide transition.

1. Direct Connection of a Coax to Waveguide(WR-42)

A coaxial to waveguide transition operating in 20GHz to 21GHz frequency range as shown in Fig. 5 is analyzed by the present interpolation scheme. The parameters used for the FDTD model are given in Table 1.

Table 1. Parameters used for the FDTD model.
(Time step: 6000, PML: 32 cell, CPU time: 320 min, 20 s)

Δx (mm)	Δy (mm)	Δz (mm)	$\Delta\rho$ (mm)	$\Delta\varphi$ (degrees)	Δt (second)
0.535	0.536	0.24	0.26	10	0.2 ps

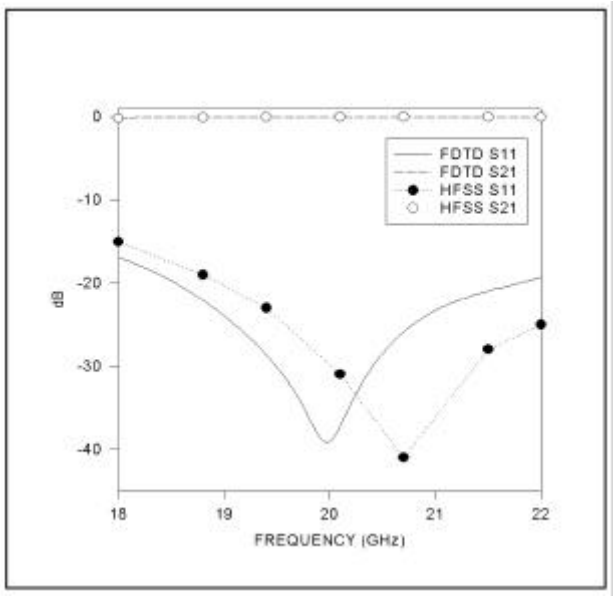

Fig. 6. Comparison between FDTD and HFSS [11] results for the geometry in Fig. 5.

The scattering parameters are calculated and compared with those of HFSS in Fig. 6. Time step used for the calculation is 6000 and 32 cell PML is adopted. The computation time is 320 minutes 20 seconds on sun sparc-20 workstation. Comparison shows that the resonant frequency of the FDTD analysis is lower than that of HFSS by 3.5%. The difference in resonance frequency is approximately 700 MHz which is not a significant discrepancy considering that the operating frequency of the transition is in 20 GHz band. Also the scattering parameter *S*11 values are well below −20 dB in most of the frequency band of interest.

2. A Ka-band Transition with SMA Connector

A Ka-band coaxial to waveguide transition using a commercially available SMA connector is designed and manufactured. The geometry is illustrated in Fig. 7 and the parameters for FDTD model are given in Table 2. The physical size of waveguide is the same as in Fig. 5.

Table 2. Parameters used for the FDTD model.
(Time step: 6000, PML: 32 cell, CPU time: 331 min, 32 s)

Δx (mm)	Δy (mm)	Δz (mm)	$\Delta \rho$ (mm)	$\Delta \varphi$ (degrees)	Δt (second)
0.535	0.536	0.24	0.21	10	0.2 ps

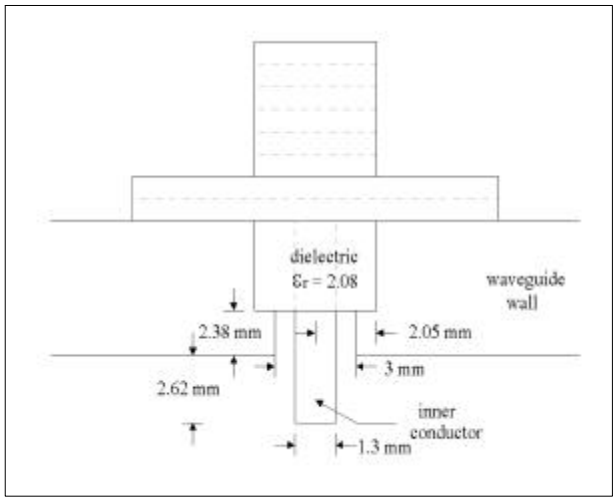

Fig. 7. Manufactured Ka-band coaxial to waveguide transition.

The s-parameters of a manufactured transition are computed using both present approach and commercial software (HFSS) and compared with those of measurement in Fig. 8.

Time step used is 6000 and 32 cell PML is applied. It takes 331 minutes 32 seconds on sun sparc-20 workstation. Comparison shows that our results match very closely to the measured values even better than HFSS results in frequency band of operation (20~21 GHz). The discrepancy possibly comes from the difference between the physical dimension and modeled dimension of a transition. Also the effect of tuning structure, which is not considered in the simulation, can be an additional factor.

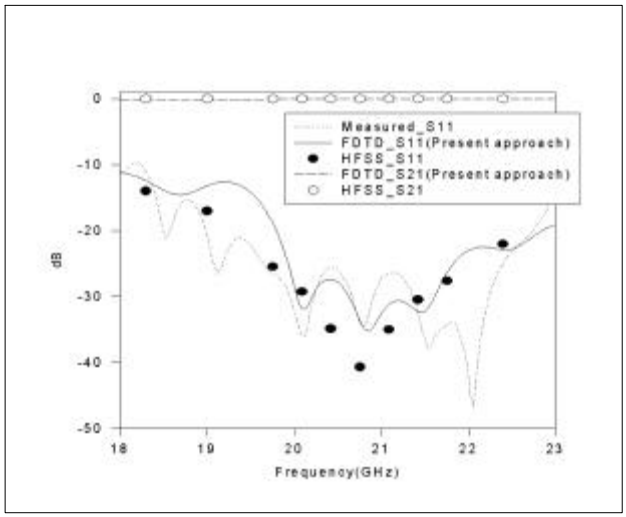

Fig. 8. Comparison of s-parameters between calculated and HFSS as well as measured data for a transition in Fig. 7.

3. A Coaxial to Waveguide Transition with a Disk Loaded Probe

A coaxial to waveguide transition with a disk-loaded probe in reference [12] is analyzed by using the present approach. Its cross sectional geometry is shown in Fig. 9 and the modeling parameters are listed in Table 3.

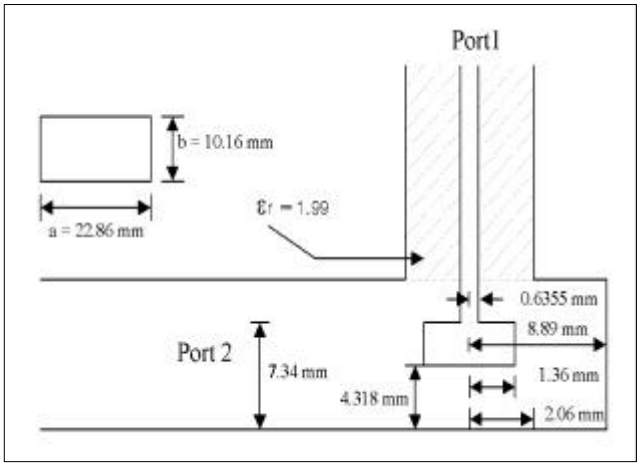

Fig. 9. Cross sectional view of a disk loaded coaxial to waveguide transition.

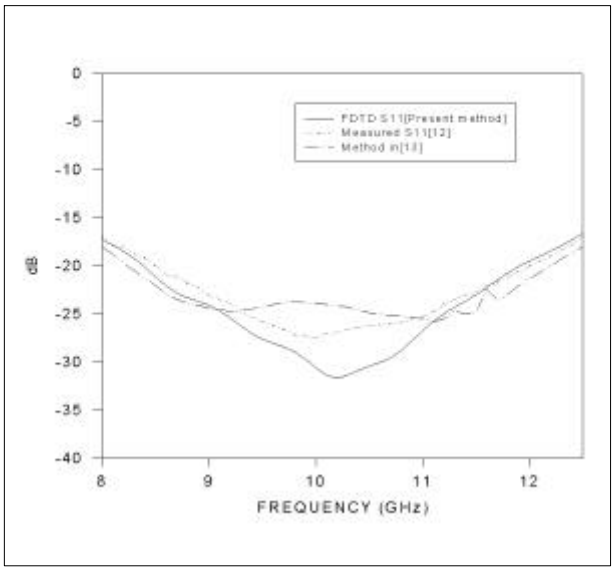

Fig. 10. Comparison between measured and theoretical results.

Table 3. Parameters used for the FDTD model.
(Time step: 8000, PML: 32 cell, CPU time: 436 min, 55 s)

Δx (mm)	Δy (mm)	Δz (mm)	$\Delta \rho$ (mm)	$\Delta \varphi$ (degrees)	Δt (second)
0.762	0.631	0.526	0.292	10	0.2 ps

In Fig. 10, we compare the calculated and measured values of *S*11 parameter for a disk loaded coaxial to waveguide transition. Time step used is 8000 and 32 cell PML is applied. The computation time required for the calculation is 436 minutes 55 seconds. In frequency band of operation 8.2 GHz to 12.4 GHz, there exists good agreement amongst the results of present approach, calculated data in [13] and measured data in [12]. Also the scattering parameter *S*11 values are well below −20dB in most of the frequency band of operation. The discrepancy between the present method and measurement might be caused by the difference between the physical dimension and modeled dimension.

IV. CONCLUSION

This paper describes a new approach, which combines the FDTD method with cylindrical to rectangular cell interpolation scheme, for analyzing a coaxial to waveguide transition. The TEM wave inside a coaxial cable is easily generated using the cylindrical FDTD method and the computer memory and calculation time can be reduced substantially over the conventional FDTD algorithm with small uniform cells. The accuracy of results increases compared with coarse uniform cell FDTD method. In the region, where the inner conductor of a coaxial cable protruding into rectangular waveguide, the FDTD with cylindrical to rectangular cell interpolation scheme is adopted for the smooth transition of electromagnetic fields from rectangular cell to cylindrical cell and vice versa. Scattering parameters are obtained for three coaxial to waveguide transition structures. First two cases are Ka-band transitions and the third one is X-band disk loaded coaxial to waveguide transition. For all three structures, the s-parameters obtained by the present approach agree very well with measured data and calculated data using HFSS and method in [12] and [13]. The interpolation scheme presented in this paper is well suited for analyzing a microwave structure with a probe near waveguide discontinuity.

In the future, the subcell method [10] suggested by Okoniewski along with the cylindrical FDTD algorithm will be investigated for the analysis of a large cylindrical microwave structure to improve the numerical efficiency of the current approach.

REFERENCES

[1] R. E. Collin, *Field Theory of Guided Waves*, New York: McGraw-Hill, 1960.

[2] A. G. Williamson, "Coaxially Fed Hollow Probe in a Rectangular Waveguide," *Proc. Inst. Elec. Eng.*, Vol. 132, Part H, 1985, pp. 273−285.

[3] K. S. Yee, "Numerical Solution of Initial Boundary Value Problems Involving Maxwell's Equations in Isotropic Media," *IEEE Trans. Antennas and Propagation*, Vol. 14, 1966, pp. 302−370.

[4] E .A. Nabarro, "T-Junction in Square Coaxial Waveguide: A FDTD Approach," *IEEE Trans. Microwave Theory Tech.*, Vol. 42, Feb. 1994, pp. 347−350.

[5] E. A. Nabarro, "Analysis of a Coupled Patch Antennas with Application in Personal Communications," *IEE Proc.*, Vol. 142, No. 6, Dec. 1995, pp. 495−497.

[6] A. Taflove and M. E. Brodwin, "Numerical Solution of Steady-State Electromagnetic Scattering Problems Using the Time-Dependent Maxwell's Equations," *IEEE Trans. Microwave Theory Tech.*, Vol. 23, Aug. 1975, pp. 623−630.

[7] J. P. Berenger, "A Perfectly Matched Layer for the Absorption of Elecromagnetic Waves," *Computational Physics*, Vol. 114, 1994, pp. 185−200.

[8] John M. Jarem, "A Method of Moments Analysis and a Finite Difference Time Domain Analysis of a Probe-Sleeve Fed Rectangular Waveguide Cavity," *IEEE Trans. Microwave Theory Tech.*, Vol. 39, Mar. 1991, pp. 444−451.

[9] Paul Y. Chung, Chen Wu, Enrique A. Navarro, and John Litva, "A Circular Mesh Scheme for the Nonorthogonal Finite Difference Time Domain Method," *IEEE AP-S*, 1995, pp. 240−243.

[10] Michal Okoniewski, "Three-Dimensional Subgridding Algorithm for FDTD," *IEEE Trans. on Antennas and Propagation*, Vol. 45, Mar. 1997, pp. 422−428.

[11] *HFSS, Ver*.5, Ansoft Corportion, Pittsburgh, PA. 15219−1119, USA.

[12] M. E. Bialkowski, "Analysis of Coaxial to Waveguide Adaptor Including a Discended Probe and a Tuning Post," *IEEE Trans., Microwave Theory Tech.*, Vol. 43, Feb. 1995, pp. 344−349.

[13] Hui-Wen, "Modeling of Generalized Coaxial Probe in Rectangular Waveguides," *IEEE Trans. Microwave Theory Tech.*, Vol. 43, Dec. 1995, pp. 2805−2810.

[14] Jan Van Hese, "Modeling of Discontinuities in General Coaxial Waveguide Structures by the FDTD-Method" *IEEE Trans. Microwave Theory Tech*., Vol. 40, Mar. 1992, pp. 547−556.

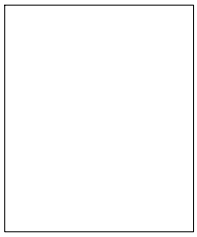

Kyung-Wan Yu received his B.S. and M.S. degrees in electronic communications engineering from Kwangwoon University, Seoul, Korea in 1991 and 1993, respectively. Since he joined ETRI in 1993, he has developed waveguide couplers, filters, and power combiners in Satellite Communications Department. His current research interests include development of MMIC circuits such as LNA, HPA, and MIXER and their applications for Ka-band microwave communication systems.

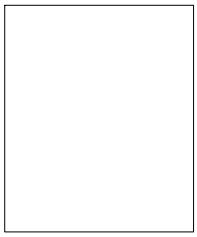

Sung-Choon Kang received his B.E. degree in electrical engineering from Seoul National University, Seoul, Korea in 1977 and M.S. and Ph.D. degrees from the Ohio State University in 1988 and 1991, respectively. Since he joined ETRI in 1991, he has been in charge of developing Ka-band Components such as LNA, SSPA using MMICs and filters for Satellite Communications. His current research interests are CMOS RFIC circuit design and its applications for mobile communication.

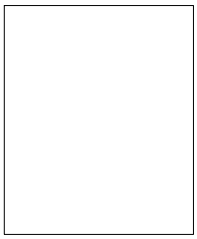

Hee-Jin Kang received the B.S. degree in telecommunication engineering from Cheju National University, Cheju, Korea, in 1996, the M.S. degree in electronic communication engineering from Hanyang University, Seoul, Korea in 1998. Since 1998, she has been pursuing the Ph.D. degree in radio science and engineering in Hanyang University. Her research interests are design and analysis of passive microwave devices.

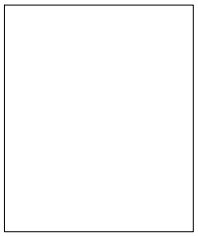

Jae-Hoon Choi received the B.S. degree in electronics engineering from Hanyang University, Seoul, Korea in 1980, the M.S. and Ph.D. degrees in electrical engineering in 1986 and 1989, respectively, both from the Ohio State University. From 1989 to 1991, he was with the Telecommunications Research Center at Arizona State University, as a research scientist. In 1991, he joined the Korea Telecom, Seoul, Korea, where he engaged in the research and development of Koreasat payload system. Since 1995, he has been with Hanyang university as an Associate professor in the division of electrical and computer engineering. His research interests include mobile and satellite communication antenna design and analysis, fullwave analysis of passive microwave device, propagation modeling and interference analysis of mobile and satellite communication systems, and EMC analysis of a high speed digital circuit. Dr. Choi has published over 25 technical papers throughout the major international journals and conferences.

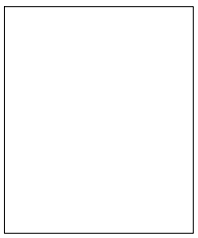

Jin-Dae Kim received the B.S. degree in ceramic engineering from Seoul National University, the M.S. in materials engineering from KAIST in 1983 and 1985 respectively. Since then, he has been working for Korea Telecom as researcher. During his work, he joined Ph.D. degree at the University of Oxford from Oct. 1991 to Jan. 1996, where he studied electronic materials as well as electron microscopy. After coming back to Korea Telecom, he has been involved in the projects related to spectrum engineering, satellite communication and so on. He is now leading a project transferring precise time/frequency using geostationary satellites.